

## Blind Color Image Steganalysis Based on Multi-Transform Combined Features Selected by a Hybrid of ANOVA and BPSO

Mansoureh Pezhmanpour  
EE Dept.  
Islamic Azad University-  
South Tehran Branch  
Tehran, Iran  
[st\\_m\\_pezhmanpour@azad.ac.ir](mailto:st_m_pezhmanpour@azad.ac.ir)

Mansour Sheikhan  
EE Dept.  
Islamic Azad University-  
South Tehran Branch  
Tehran, Iran  
[msheikhn@azad.ac.ir](mailto:msheikhn@azad.ac.ir)

M. Shahram Moin  
Multimedia Sys. Group  
IT Dept.  
Iran Telecom Research Center  
Tehran, Iran  
[moin@itrc.ac.ir](mailto:moin@itrc.ac.ir)

Received: July 20, 2010 – Accepted: September 5, 2010

**Abstract**— Steganalysis techniques have been classified into two major categories: blind steganalysis which is independent of the steganography method and specific steganalysis which attempts to detect specific steganographic media. Feature extraction is an important functional block in the steganalysis systems. The features are commonly in spatial domain or extracted from transform domains such as discrete wavelet transform (DWT), discrete cosine transform (DCT) or contourlet transform (CT). In this paper, a blind color image steganalysis method based on a hybrid set of features (statistical moments, entropy, and co-occurrence matrix features) extracted from a combination of DWT, DCT, and CT is proposed. The hybrid of “analysis of variation (ANOVA)” as an open-loop feature selection method, and “binary particle swarm optimization (BPSO)” as a closed-loop one, is used in this work to improve the detection rate in tandem with significant reduction in the size of feature set. Jsteg, OutGuess, JPHS and model-based steganography methods are attacked in this work. By using the hybrid of “ANOVA+BPSO”, the number of features is reduced to 13. Empirical results show that the most discriminative features in clean/stego image classification are statistical moments of co-occurrence matrix of contourlet transform. The most discriminative selected features are fed into a nonlinear support vector machine (SVM) classifier to distinguish the cover and stego images. Average detection accuracy of the proposed model is above 81 percent for the embedding-rate ranges of 5% to 25%.

**Keywords**- Steganalysis, entropy, statistical moments, DCT, DWT, contourlet, co-occurrence matrix

### I. INTRODUCTION

Steganography is the art of hiding information in a cover media such as image, so that it is not detected visually. On the other hand, steganalysis is used to detect whether a message is hidden or not in a media [1]. Steganalysis methods have been classified into two major categories: blind steganalysis and specific steganalysis. The blind steganalysis is independent of the steganography method. The specific steganalysis attempts to detect specific steganographic media. Generally, the steganalysis procedure consists of three functional stages: feature extraction, feature selection,

and classification. Features are extracted directly from the spatial domain or from a transform domain such as discrete wavelet transform (DWT), discrete cosine transforms (DCT), or contourlet transform (CT). In this work, the combined set of features based on DCT, DWT and CT are used as the extracted features. Also, a hybrid feature selection method based on "analysis of variation (ANOVA)" and "binary particle swarm optimization (BPSO)" is proposed to reduce efficiently the feature-space dimension. In this way, the proposed system offers acceptable average detection accuracy for stego images with low embedding rates (below 25%) of steganography method's capacity.

The block diagram of the proposed steganalysis model in this work is illustrated in Figure 1. As shown in Figure 1, steganalysis is based on the features that are extracted from two usual transformations (DCT and DWT) and contourlet transform which is a more recent transformation used in steganalysis [2]. The extracted features are as follow: entropy, co-occurrence matrix, and statistical moments (mean, variance, skewness, and kurtosis). The ability of features in discriminating stego and clean images is evaluated by ANOVA technique. In order to reduce the dimension of feature space, ANOVA is used as an open-loop feature selector (independent of classifier) and BPSO is also used as a closed-loop selection method in this study. Support vector machine (SVM) is used to report the specificity and sensitivity of the proposed steganalysis system.

This paper is organized as follows. The related works are described in the next section. In Section III, the transformations and features, which are used in this work, are reviewed briefly. ANOVA and BPSO feature selection algorithms are introduced in Section IV. SVM classifier is presented briefly in Section V. The details of dataset and attack types are discussed in Section VI. Empirical results are reported in Section VII. The discussions and conclusions are also provided in Section VIII and IX, respectively.

## II. RELATED WORKS

Some of the researches in blind steganalysis are as follow: Avcibas et al. [3] have proposed a blind steganalysis method based on the image quality metrics and used ANOVA technique to select the most significant features. They have used multivariate regression analysis for classification. Xuan et al. [4] have proposed a steganalysis method that is based on the statistical moments of characteristic functions of wavelet subbands. They have shown that the moments in the characteristic function domain are more sensitive to data hiding than moments in histogram domain. Bayes classifier has been used in their proposed method. Lyu and Farid [5] have used statistical-model features including first-order and higher-order magnitude and phase statistics from wavelet and local angular harmonic decompositions. They have used three types of classifiers: linear SVM, nonlinear SVM and one-class SVM. Wang and Moulin [6] have used empirical moments of probability density functions (PDFs) and empirical characteristic function (CF) moments of the PDFs in different wavelet subband coefficients and their cross-subband prediction errors. In their work, Bhattacharyya distance has been used for feature evaluation to improve the classification performance. They have shown that CF moments of subband histogram are more sensitive to embedding rate than PDF moments of subband coefficients. For the prediction-error subband, the PDF moments are better features than CF moments. Pevny and Fridrich [7] have used a merging feature set of DCT and calibrated Markov features and also SVM multi-classifier for images with different quality factors. Qin et al. [8] have used Moulin's and Fridrich's features and proposed principal feature selection and fusion (PFSF) method to reduce the number of features. They have used a linear transform

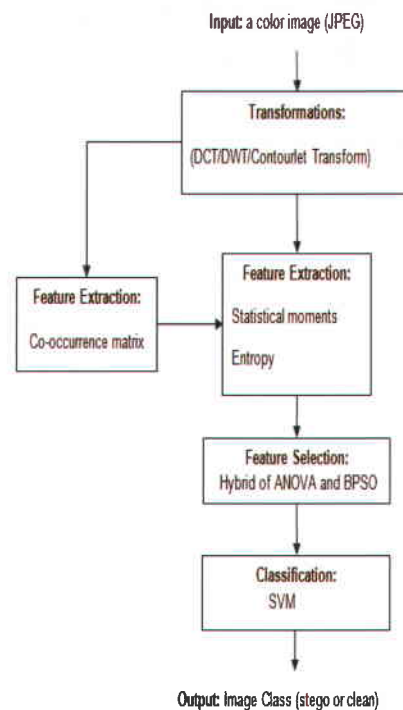


Figure 1. Block diagram of the proposed steganalysis method

based on principal components analysis (PCA) and Savage decision making to eliminate insignificant features, then fused the selected features, followed by selecting the principal features from the fused features to form a new feature set. Sajedi and Jamzad [2] have used statistical moments of eight subbands in the third level of contourlet and the statistical moments of difference between actual and linear predicted coefficients of contourlet as the features.

## III. TRANSFORMATIONS AND FEATURE EXTRACTION METHODS

In this study, each image is first transformed to other domains through three types of transformations (Fig. 1): DCT [9], DWT [10] (in 3 levels), and CT [11] (in 3 levels). Four statistical moments (mean, variance, skewness, and kurtosis) are extracted from the transformed images and their co-occurrence matrices are calculated. Also, irregularity of the transformed images is quantified using Shannon entropy (described in Part B of this section).

### A. Transformations

In this study, the performance of three transformations is investigated in the proposed steganalysis method: DCT, DWT, and CT. It is noted that the output of wavelet transform contains multiple resolutions of space points at desired frequencies; however, it has limited directional information. Two-dimensional DWT offers a decomposition of approximation coefficients of each level into four components: the approximation, and the details only in three orientations (horizontal, vertical, and diagonal). The features are extracted from the subband coefficients at each level of decomposition. On the other hand, in the contourlet transform more

directional information can be captured by decomposing an image into directional subimages at different scales. So, this transform can capture heterogeneities and smooth contours more accurately than DWT. In other words, contourlet is a multi-scale and multi-direction transformation.

Contourlet includes two major parts: Laplacian pyramid and directional filter banks. The Laplacian pyramid produces multi-scale decomposition. On the other hand, the directional filter banks produce multi-direction decompositions.

The Laplacian pyramid decomposition, at each level, generates a down-sampled lowpass version of the original and the difference between original and prediction signals. The directional filter banks contain two serial building blocks. The first building block is a two-channel quincunx filter bank with fan filters that divides a 2-D spectrum into two directions: horizontal and vertical. The second building block of directional filter banks is a shearing operator, which amounts to reordering of image samples [11].

Contourlet filter bank is a combination of a Laplacian pyramid and a directional filter bank. Figure 2 shows contourlet filter bank in one level. First the bandpass images from the Laplacian pyramid enter into a directional filter bank so that directional information can be captured. This scheme can be iterated on the coarse image. This combination is a double iterated filter bank structure, which decomposes images into directional subbands at multiple scales. In this study, the discrete contourlet transformation is applied to images in 3 levels and 8 directions.

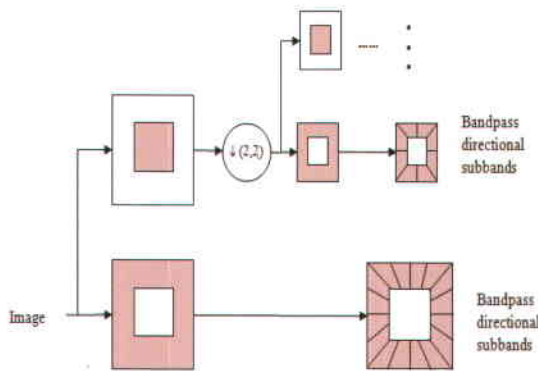


Figure 2. Contourlet filter bank [11]

**B. Features**

Four moments (mean, variance, skewness, and kurtosis) are used as statistical features in this study.

$$M(x) = \frac{1}{n} \sum_{k=1}^n x_k \tag{1}$$

$$Var(x) = \frac{1}{n-1} \sum_{i=1}^n (x_i - M(x))^2 \tag{2}$$

$$S(x) = E \left[ \left( \frac{x - M(x)}{\sqrt{Var(x)}} \right)^3 \right] \tag{3}$$

$$K(x) = E \left[ \left( \frac{x - M(x)}{\sqrt{Var(x)}} \right)^4 \right] \tag{4}$$

These features are applied to DCT, DWT and CT domains.

Entropy measurements quantify the irregularity of a system or signal. Since hiding information into a cover may result to increased irregularity and noisiness of the stego data in spatial domain or frequency domain, it seems that entropy is an appropriate candidate feature for steganalysis. In addition, since contourlet is involved in both spatial or frequency domains and it is much sensitive to edges, that is mostly more affected by the hidden data, entropy of contourlet is more effective for steganalysis [12].

For this purpose, Shannon entropy is an effective statistical method of measuring entropy. It is computed in the following way:

$$ENT = - \sum_i P_i \log(P_i) \tag{5}$$

where  $P_i$  is the probability of a pixel having intensity in the  $i^{th}$  quantized level.

By using co-occurrence matrix, other groups of features are extracted in this study. These features are as follow: energy, variance, skewness, and kurtosis. It is noted that co-occurrence matrix is defined over an image as the distribution of co-occurring values at a given offset. Mathematically, a co-occurrence matrix  $C$  is defined over an  $n \times m$  image  $I$ , parameterized by an offset  $(\Delta x, \Delta y)$ , as follows:

$$C_{\Delta x \Delta y}(i, j) = \sum_{p=1}^n \sum_{q=1}^m \begin{cases} 1 & I(p, q) = i \text{ and } (p + \Delta x, q + \Delta y) = j \\ 0 & ; \text{ otherwise} \end{cases} \tag{6}$$

The value of image is originally referred to the gray scale level of a specified pixel [13]. In this study, the co-occurrence matrix is applied to the transformed images by contourlet transform, DCT, and DWT (with 16 grayscale). The co-occurrence matrix is determined using a set of 4 offsets sweeping through 180 degrees (i.e. 0, 45, 90, and 135 degrees) at the same distance to achieve a degree of rotational invariance. The energy feature of co-occurrence matrix is calculated as follows:

$$Energy = \sum_{i, j} \{ C(i, j) \}^2 \tag{7}$$

Also, other statistical features (variance, skewness, and kurtosis) are extracted from co-occurrence matrix of DCT, DWT and CT domains.

**IV. FEATURE SELECTION**

In this study, two methods are used for feature selection in a hybrid form: one-way ANOVA, for open-loop feature selection, and BPSO [14] for closed-loop feature selection. One-way ANOVA evaluates the discrimination ability of features in discriminating groups individually by ignoring their correlation. Considering correlations may reveal a group of features which are discriminative together, but are not discriminative separately. When we have several features, BPSO may not converge easily to select a number of significantly discriminative interacted features, due to high computational load. In this study, ANOVA selects a number of individually discriminative features at the first stage, and then the



BPSO is used to select a set of more effective features among them.

A. Analysis of Variance

ANOVA is a statistical method that is widely used to evaluate the feature set abilities in discriminating two or more classes. The discrimination is based on the variations both between and within classes indicated by an index, called *p*-value. This value is between 0 and 1. Strong or weak ability of the features in discrimination corresponds to a *p*-value close to 0 and 1, respectively. The *p*-value is computed through *F*-test which is a ratio of “between-group variation” to “within-group variation”. Larger *F* means more difference between groups than within groups. It is noted that one-way ANOVA investigates discrimination of groups based on only one feature (by ignoring the interactions with other features).

In this study, one-way ANOVA is used as an open-loop feature selection approach for selecting discriminative features in the context of distinguishing stego from clean images. Indeed, the ANOVA constructs a feature space for BPSO. The number of selected features by ANOVA should not be too large that leads to divergence of BPSO algorithm. On the other hand, it should not be too small that leads to dimensionally limited feature space for selecting features by BPSO. In this way, *p*-value and *F* thresholds are set experimentally. Features with *p*-values less than  $10^{-5}$  and  $F > 15$  are selected as the most discriminative features in this step.

B. Binary Particle Swarm Optimization

Particle swarm optimization (PSO) is a population-based algorithm to find solutions of an optimization problem. The search space is constructed based on the variables of problem. In BPSO, since the variables indicate existence or non-existence of a feature, the search space is a binary space. Positions of the particles are updated based on updating their velocity according to the following equations:

$$v_{ij}(t+1) = wv_{ij}(t) + C_1R_1(p_{best_{ij}} - x_{ij}(t)) + C_2R_2(g_{best_j} - x_{ij}(t)) \quad (8)$$

$$x_{ij}(t+1) = x_{ij}(t) + v_{ij}(t+1) \quad (9)$$

where  $v_{ij}(t)$  indicates the velocity of  $j^{th}$  component of  $i^{th}$  particle at the position  $x_{ij}(t)$  in  $t^{th}$  iteration.  $w$  is the velocity coefficient,  $R_1$  and  $R_2$  are two random numbers.

$p_{best_{ij}}$  is the  $j^{th}$  component of  $i^{th}$  particle which minimizes the cost function as compared to the previous iterations.  $g_{best_j}$  indicates the  $j^{th}$  component of the best particle in minimization of cost function in comparison to the previous iterations.  $C_1$  and  $C_2$  are the weights of local and global terms of search algorithm. Figure 3 illustrates the flowchart of PSO algorithm. The conversion of continuous PSO to BPSO is performed as follows:

$$\begin{aligned} x_{ij}(t+1) &= 0; rand() \geq S(v_{ij}(t+1)), \\ x_{ij}(t+1) &= 1; rand() < S(v_{ij}(t+1)) \end{aligned} \quad (10)$$

$$S(v_{ij}(t+1)) = \frac{1}{1 + e^{-v_{ij}(t+1)}} \quad (11)$$

where  $S$  is the sigmoid function. In this way, the continuous positions are converted to binary positions. Binary position “1” is assigned to effective features and binary position “0” to non-effective features in distinguishing stego from clean images.

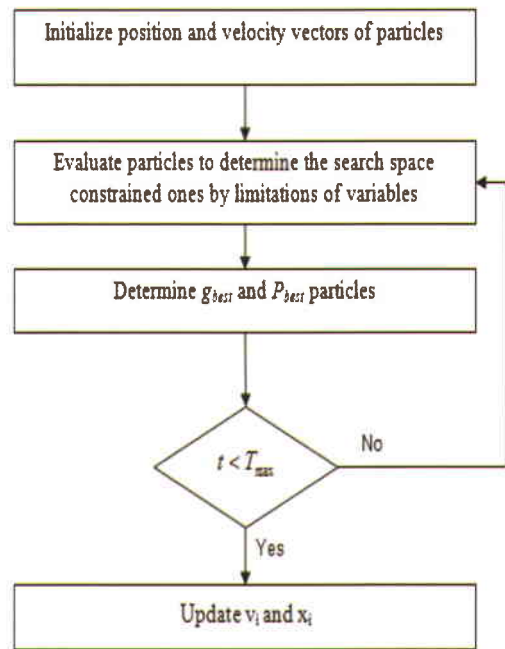


Figure 3. Flowchart of the PSO algorithm [14]

V. CLASSIFICATION METHOD

The support vector machine (SVM) [15-17] is a supervised learning method that is used for classification. It works based on the construction of a separating hyperplane which maximizes the margin between the input data classes that are viewed in an *n*-dimensional feature space. Also, the hyperplane may be formed according to a kernel. An SVM with Gaussian radial basis function (RBF) kernel is used in this paper:

$$k(x_i, x_j) = \exp\left(-\frac{\|x_i - x_j\|^2}{2\sigma^2}\right) \quad (12)$$

We used  $\nu$ -soft margin support vector classifier ( $\nu$ -SVC) in which a parameter,  $\nu$ , controls the number of support vectors and training errors [17]. The value of  $\nu$  is in the (0, 1] interval that is an upper bound on the fraction of training errors and a lower bound on the fraction of support vectors.

VI. DATASET

The Uncompressed Color Image Database (UCID) is used in this study [18]. This database contains 1338 color TIFF images. The images have been converted



[Downloaded from journal.ijict.ac.ir on 2024-04-20]

Table 1. Selected features by ANOVA

Transformation		Mean		Skewness		Kurtosis		Shannon Entropy	
		<i>p-value</i>	<i>F</i>	<i>p-value</i>	<i>F</i>	<i>p-value</i>	<i>F</i>	<i>p-value</i>	<i>F</i>
<b>DCT</b>		NS	NS	$1.10 \times 10^{-8}_R$	30.54	$2.31 \times 10^{-8}_R$	29.67	$1.43 \times 10^{-6}_R$	15.05
<b>DWT</b>	<b>L3</b>	$9.21 \times 10^{-9}_B$	52.73	NS	NS	$5.42 \times 10^{-6}_R$	19.04	$1.60 \times 10^{-7}_R$ $0_B$	22.03 90.06
	<b>L1</b>	NS	NS	NS	NS	NS	NS	NS	NS
<b>CT</b>	<b>L2</b>	$5.07 \times 10^{-6}_R$ $0_R$	16.83 47.75	$1.04 \times 10^{-6}_R$	46.05	NS	NS	NS	NS
	<b>L3</b>	$3.82 \times 10^{-11}_R$	35.21	$0_R$	81.87	$0_R$	<b>85.48</b>	$1.24 \times 10^{-10}_R$	<b>52.01</b>
		$0_R$	<b>86.43</b>	$0_R$	<b>92.67</b>	$3.50 \times 10^{-9}_B$	70.67		
$0_R$		<b>129.23</b>	$0_G$						
		$0_B$	108.99						

Note: R, G and B indices indicate the corresponding color channel. NS stands for "not selected" and  $L_i$  is the  $i^{th}$  level of transform. Selected features by BPSO, at the next step, are highlighted.

Table 2. Selected co-occurrence matrix-based features by ANOVA

Transformation		Energy		Variance		Skewness		Kurtosis	
		<i>p-value</i>	<i>F</i>	<i>p-value</i>	<i>F</i>	<i>p-value</i>	<i>F</i>	<i>p-value</i>	<i>F</i>
<b>DCT</b>		NS	NS	$1.03 \times 10^{-6}_R$	18.01	NS	NS	NS	NS
<b>DWT</b>	<b>L3</b>	NS	NS	$5.34 \times 10^{-7}_G$	23.67	NS	NS	$2.76 \times 10^{-6}_R$	15.48
	<b>L1</b>	$1.06 \times 10^{-8}_B$	20.00	NS	NS	$1.42 \times 10^{-6}_R$	15.01	$0_B$	31.59
<b>Contourlet</b>	<b>L2</b>	$2.54 \times 10^{-7}_B$	18.54	$1.30 \times 10^{-9}_R$	<b>30.07</b>	$2.05 \times 10^{-6}_B$	17.51	$4.23 \times 10^{-8}_R$	33.06
		$0_R$	<b>64.98</b>	$3.57 \times 10^{-6}_B$	17.74				
	<b>L3</b>	$6.82 \times 10^{-18}_G$	35.27	$7.30 \times 10^{-6}_R$	15.93	$9.90 \times 10^{-7}_R$	21.08	$0_R$	<b>61.71</b>
		$0_R$	<b>70.04</b>	$1.12 \times 10^{-9}_R$	<b>40.26</b>	$0_B$	56.88		
		$0_R$	<b>88.65</b>	$1.53 \times 10^{-7}_B$	22.02				
		$0_B$	<b>62.42</b>						
		$0_G$	<b>50.28</b>						

Note: R, G and B indices indicate the corresponding color channel. NS stands for "not selected" and  $L_i$  is the  $i^{th}$  level of transform. Selected features by BPSO, at the next step, are highlighted.

VII. EXPERIMENTAL RESULTS

from TIFF to JPEG images with a quality factor of 80, in order to be used with steganographic methods. In order to construct stego dataset, Jsteg [19], Outguess [20], Model-based algorithm [21] and JPHE software [22] have been applied to the JPEG images to embed the randomly created secret message. So, four groups of stego images are generated, each with the size of 1338 color JPEG images. The mentioned four groups are mixed and 1338 stego images are selected randomly, with approximately equal number of selected images from each group. The size of message is considered to be 5%, 10% and 25% of embedding capacity of Jsteg, Outguess and model-based methods.

A total of 2676 images, 1338 stego images and 1338 cover images, have been used in our experiments. In this work, 120 features of contourlet (3 scales, 8 directions), 20 wavelet-based features (in 3 levels), 5 DCT-based features, 480 features obtained from co-occurrence matrices of contourlet and 100 features from co-occurrence matrices of DCT and DWT have been used. Consequently, a feature vector containing 725 components per color has been obtained. The one-way ANOVA selected 42 features as follow: 19 features that were statistical moments and entropy of the transformed images (Table 1), and 23 features that were statistical moments of co-occurrence matrices (Table 2).



As shown in Table 1, the most discriminative features are selected from contourlet transformation in comparison to DCT and DWT. Contourlet captures the heterogeneities and smooth contours more accurately than DCT and DWT. As shown in Table 2, the energy of co-occurrence matrix of contourlet transform is significantly sensitive to data hiding. As noted earlier, the selected features by BPSO are highlighted in Table 1 and Table 2. So, the hybrid of ANOVA and BPSO has selected 13 features. Random sub-sampling validation has been used as the cross validation method. In this work, 80% of data is selected randomly for training and the remained 20% for test. The SVM classifier has been trained separately for each of 25%, 10%, and 5% embedding rates. The detection accuracy of the proposed steganalysis method for different embedding rates of four steganography methods is reported in Table 3. Also, the classification results, in terms of confusion matrix, are reported in Table 4.

Figure 4 shows the receiver operating characteristic (ROC) curves which denotes the percentage of correctly detected stego images (True Positive/TP) versus the percentage of cover images detected as stego (False Positive/FP).

#### VIII. DISCUSSIONS

The performance and specifications of the proposed steganalysis method are compared to similar works in Table 5. It is noted that, because of the diversity of steganography methods and various number of images and payloads in other related works, the fair comparison is a hard task. In this way, Lyu and Farid [5] have employed statistical-model features consists of first-order and higher-order magnitude and phase statistics from wavelet and local angular harmonic decompositions (LAHD) which result in 432 features. They achieved maximum detection accuracy of 78.2% for embedding rate of 100% and minimum of 7.8% for 5% embedding rate. So, the detection accuracy of clean images has been greater than 99%. Pevny and Fridrich [7] have used 274-dimensional feature vector based on the incorporation of calibrated Markov features and DCT feature set to attack to F5, Outguess, model-based, JP Hide & Seek, and Steghide steganography methods. The detection accuracies in that work have been above 92% for embedding rates above 25%. Rodriguez et al. [23] have extracted higher-order statistics and predicted log errors from energy bands of the modified-DCT transform. They have used 120 features and attacked to the output of steganography methods with embedding rates of 5% to 25%. They have achieved higher accuracy with Parzen-window in comparison to SVM.

The above mentioned steganalysis method has been based on DCT and wavelet coefficients and the size of feature vector was more than 120. The wavelet packet decomposition of images based on the Shannon entropy information cost function has been performed in [24] and high order absolute characteristic function moments of histogram extracted from the coefficient subbands have been obtained. The number of features in [24] has been reduced to 39 as reported in Table 5. Back-propagation (BP) neural network has been used as the classifier of this method. The average detection accuracy of 92% has been achieved in [24]. It is noted that the natural images have been replicated until the amount of natural images be equal to the amount of stego images in [24] and this may increase the detection accuracy as compared to 1338 randomly selected stego images in our work.

We extract the features from CT in addition to DCT and DWT in this work. It is noted that most of the features selected by BPSO and ANOVA are from CT domain. As shown in Table 5, the size of feature set is reduced significantly in the proposed method by employing efficient feature selection techniques and the average detection accuracy of proposed method is comparable with similar works, as well. The advantages of the proposed method are significant reduction of feature numbers and using a hybrid feature selection approach by employing ANOVA and BPSO as open- and closed-loop feature selection methods. It is noted that using only ANOVA does not result in high classification rates. Also, using only BPSO will result in high computational load. Then, employing the hybrid approach will result in improved classification rates, in comparison to similar works, with reasonable computational load. The disadvantage of proposed method is that extracting contourlet transform domain features has high computational complexity in comparison to other features. Also, BPSO feature selection is a time-consuming algorithm.

#### IX. CONCLUSIONS

The main functional blocks in blind steganalysis are feature extraction and classification. Feature extraction is a more interesting topic and has been investigated more in comparison to classification subject. However, both of these blocks have been investigated in this research. A combination of three usual transformations (DCT, DWT and CT) has been used to offer a complete set of features. In this way, the proposed feature selection method has a wider range of features to select the best candidates.

Table 3. Detection accuracy of the proposed steganalysis method for 25%, 10% and 5% embedding rates

Steganography methods	Outguess			Jsteg			JPHS			Model-Based		
	5%	10%	25%	5%	10%	25%	5%	10%	25%	5%	10%	25%
Embedding rate	5%	10%	25%	5%	10%	25%	5%	10%	25%	5%	10%	25%
Detection accuracy (%)	84.61	87.53	97.12	82.10	86.09	95.39	75.33	78.45	91.73	79.22	84.86	93.85





Table 4. Confusion matrix of the proposed steganalysis method for 25%, 10% and 5% embedding rates

Predicted \ Actual	Embedding rate (%)					
	25		10		5	
	Stego	Clean	Stego	Clean	Stego	Clean
Stego	96.83	7.42	87.47	15.13	81.29	18.62
Clean	3.17	92.58	8.53	84.87	18.71	81.38

Table 5. Performance comparison of the proposed steganalysis method and similar works

Steganalysis method	Steganography method	Number of features	Classifier	Average detection accuracy
Lyu and Farid [5]	Jsteg, Outguess, Steghide, Jphide, F5	432	SVM	78.2%, 64.5%, 37.0%, and 7.8% for embedding rates of 100%, 78%, 20%, and 5%
Pevny and Fridrich [7]	F5, Outguess, Model-based, JP Hide & Seek, Steghide	274	SVM	Above 92% for embedding rates above 25%
Rodriguez et al. [23]	F5, Jphide, Jsteg, Model-based, Outguess, Steghide	120	Parzen-window, SVM	Parzen-window: 93%, SVM: 85% for embedding rates of 5% to 25%
Yang et al. [24]	LSB, Jphide, Jsteg, F5	39-255	BP Neural Network	92% for 256×256, 128×128 and 64×64 secret image sizes
Proposed method	Jsteg, Outguess, JPHS, Model-based	13	SVM	81%, 86%, and 94% for embedding rates of 5%, 10%, and 25%

A set of statistical and entropy-based features have been extracted directly from the transformed images. The indirect statistical and entropy-based features of co-occurrence matrices of the transformed images have been extracted, too. In this way, 725 features (per color) have been extracted from the mentioned transformations and SVM has been used to distinguish stego from cover images. In order to reduce the computational load and to improve the accuracy rate of classification, the number of features has been reduced. As an innovative suggestion, a hybrid structure of ANOVA and BPSO has been used as the feature selection method in this work. ANOVA has selected 42 features in the first stage and then 13 features have been selected by BPSO. Empirical results have shown that most of the features are based on the contourlet transformation. Also, the energy of co-occurrence matrix of contourlet transform and the mean of contourlet coefficients of the third level are more sensitive to data hiding than other statistical features. The detection accuracy of the proposed system in low embedding rates, with a significantly reduced feature set size, is comparable with similar works.

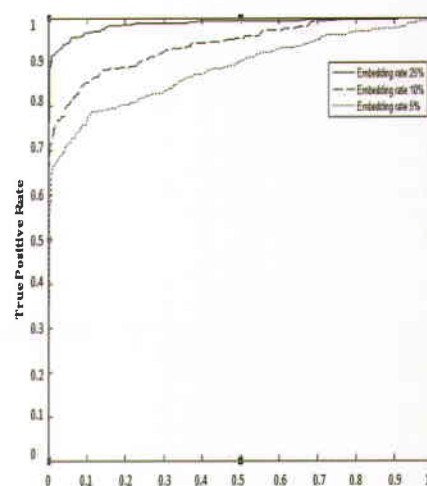


Figure 4. ROC curves of proposed steganography method for three embedding rates

## REFERENCES

- [1] A. Nissar, and A. H. Mir, "Classification of steganalysis techniques: A study," *Digital Sign. Process.*, vol. 20, pp. 1758-1770, 2010.
- [2] H. Sajedi, and M. Jamzad, "CBS: Contourlet-based steganalysis method," *J. Sign. Process. Syst.*, vol. 61, pp. 367-373, 2010.
- [3] I. Avcibas, N. Memon, and B. Sankur, "Steganalysis using image quality metric," *IEEE Trans. Image Process.*, vol. 12, pp. 221-229, 2003.
- [4] G. R. Xuan, Y. Q. Shi, J. J. Gao, D. K. Zou, C. Y. Yang, Z. P. Zhang, P. Q. Chai, C. H. Chen, and W. Chen, "Steganalysis based on multiple features formed by statistical moments of wavelet characteristic functions," *Proc. 7<sup>th</sup> Int. Information Hiding Workshop, Lecture Notes in Computer Science*, vol. 3727, pp. 262-277, 2005.
- [5] S. Lyu, and H. Farid, "Steganalysis using higher-order image statistics," *IEEE Trans. Inf. Forens. Secur.*, vol. 1, pp. 111-119, 2006.
- [6] Y. Wang, and P. Moulin, "Optimized feature extraction for learning-based image steganalysis," *IEEE Trans. Inf. Forens. Secur.*, vol. 2, pp. 31-45, 2007.
- [7] T. Pevny, and J. Fridrich, "Markov and DCT features for multi-class JPEG steganalysis," *SPIE-IS & T Electronic Imaging Journal*, vol. 650503: 1-13, 2007.
- [8] J. Qin, X. Sun, X. Xiang, and C. Niu, "Principal feature selection and fusion method for image steganalysis," *Journal of Electronic Imaging*, vol. 18, pp. 1-14, 2009.
- [9] R. Reininger, and J. Gibson, "Distributions of the two-dimensional DCT coefficients for images," *IEEE Trans. Commun.*, vol. 31, pp. 835-839, 1983.
- [10] S. G. Mallat, "A theory for multiresolution signal decomposition: The wavelet representation," *IEEE Trans. Patt. Anal. Mach. Intell.*, vol. 11, pp. 674-693, 1989.
- [11] M. N. Do, and M. Vetterli, "The contourlet transform: An efficient directional multiresolution image representation," *IEEE Trans. Image Process.*, vol. 14, pp. 2091-2106, 2005.
- [12] M. Ferraro, G. Boccignone, and T. Caelli, "Entropy-based representation of image information," *Patt. Recog. Lett.*, vol. 23, pp. 1391-1398, 2002.
- [13] J. F. Haddon, and J. F. Boyce, "Co-occurrence matrices for image analysis," *Electron. Commun. Eng. J.*, vol. 5, pp. 71-83, 1993.
- [14] S. Lee, S. Soak, S. Oh, W. Pedrycz, and M. Jeon, "Modified binary particle swarm optimization," *Prog. Natur. Sci.*, vol. 18, pp. 1161-1166, 2008.
- [15] C. Cortes, and V. Vapnic, "Support-vector networks," *Mach. Learn.*, vol. 20, pp. 273-297, 1995.
- [16] Y. Shihong, L. Ping, and H. Peiyi, "SVM classification: Its contents and challenges," *Appl. Math. J. Chinese Univ. Ser. B*, vol. 18, pp. 332-342, 2003.
- [17] J. C. Chang, and C. J. Lin, LIBSVM: A library for support vector machines, 2001 (Available on: <http://www.csie.ntu.edu.tw/~cjlin/libsvm>).
- [18] G. Schaefer, and M. Stich, "UCID: An uncompressed colour image database," *Proc. SPIE, Storage and Retrieval Methods and Applications for Multimedia*, pp. 472-480, 2004 (Available on: <http://vision.cs.aston.ac.uk/datasets/UCID/ucid.html>).
- [19] D. Upham, Jsteg Steganographic Algorithm, 1999 (Software available on: <ftp://ftp.funet.fi/pub/crypt/steganography>).
- [20] N. Provos, Outguess-Universal Steganography, 1998 (Software available on: <http://www.outguess.org>).
- [21] P. A. Sallee, Model-Based Steganography, 2003 (Software available on: <http://www.philsallee.com/mbsteg/index.html>).
- [22] JPHS Steganography Software, 2008 (Software available on: [http://www.filewatcher.com/m/jphs\\_05.zip.184359.0.0.html](http://www.filewatcher.com/m/jphs_05.zip.184359.0.0.html)).
- [23] B. Rodriguez, M. Gilbert, L. Peterson, and S. S. Agaian, "Steganography anomaly detection using simple one-class classification," *Proc. SPIE*, vol. 65790E, pp. 1-9, 2007.
- [24] L. X. Yang, L. FenLin, Y. ChunFang, and W. DaoShun, "Image universal steganalysis based on best wavelet packet

decomposition," *Sci. in China Ser. F: Inform. Sci.*, vol. 53, pp. 634-647, 2010.



image processing, steganography and steganalysis techniques, and bioinformatics.



**M. Shekhan** received the B.Sc. degree in electronic engineering from Ferdowsi University, Meshed, Iran, in 1988 and his M.Sc. and Ph.D. degrees in communication engineering from Islamic Azad University, Tehran, Iran, in 1991 and 1997, respectively. He is currently an Associate Professor in Electrical Engineering Department of Islamic Azad University-South Tehran Branch. His research interests include intelligent systems, signal processing, and neural networks. Dr. Shekhan has published more than 40 journal and 90 conference papers in the two recent decades.



**M. Shahram Moin** received his B.Sc. degree in electrical engineering from Amir Kabir University of Technology, Tehran, Iran, in 1988, M.Sc. degree in electrical engineering from Tehran University, Tehran, Iran, in 1991, and Ph.D. degree in electrical engineering from École Polytechnique de Montréal, Montréal, Canada, in 2000.

From 2000 to 2001, he worked as Research Associate in Scribens Laboratory, École Polytechnique de Montréal, Montréal, Canada and has been involved in the research on dynamic handwritten document processing. From 2001 to 2004, he has been the project manager of biometric systems, and from 2004 till now, he is the Head of the Multimedia Research Group at Iran Telecommunication Research Center, Tehran, Iran.

Dr. Moin is assistant professor and lecturer of Artificial Neural Networks, Digital Signal Processing, Pattern Recognition and Stochastic Processes courses in graduate levels. He has published 12 journal papers, 7 book chapters and 60 conference papers.

Dr. Moin is an IEEE Senior member and also member of the directing board of IEEE Iran Section and Iranian Society of Machine Vision & Image Processing.

His current research interests are applications of image processing, signal processing and pattern recognition in multimedia information security (including biometric systems and multimedia watermarking), multimedia information retrieval, human-computer interaction systems and multimedia information coding.

